Polycyclic aromatic hydrocarbons as finite size models of graphene and graphene nanoribbons: enhanced electron density edge effect. Chem Phys

ARTICLE *in* NATIONAL ACADEMY SCIENCE LETTERS · APRIL 2012

Impact Factor: 0.29 · DOI: 10.1016/j.chemphys.2012.04.005

Chemical Physics 402 (2012) 56–68

Contents lists available at SciVerse ScienceDirect

Chemical Physics

journal homepage: www.elsevier.com/locate/chemphys

Polycyclic aromatic hydrocarbons as finite size models of graphene and graphene nanoribbons: Enhanced electron density edge effect

P.C. Mishra *, Amarjeet Yadav

Department of Physics, Banaras Hindu University, Varanasi 221 005, India

ARTICLE INFO

Article history:
Received 4 January 2012
In final form 4 April 2012
Available online 16 April 2012

Keywords:
Graphene
Graphene nanoribbons
Edge effect
Reactivity
Electron density

ABSTRACT

Distinct edge effects on physical and chemical properties are known to exist in graphene and graphene nanoribbons (GNRs). The present study provides a clue to understand the origin of these effects in terms of electron density distribution. Continuous electron density, molecular electrostatic potential and net charges obtained using density functional theory in several polycyclic aromatic hydrocarbons (PAHs) taken as finite size models of graphene and GNRs are analyzed. Electron density is found to be enhanced at the edges in comparison to those in the other parts of several PAHs and a similar distribution is also shown by spin densities in triplet ground states. Electron density is enhanced even at the hydrogen passivated internal edges created by removing carbon atoms of an inner benzene ring. Various experimental observations relating to distinct properties of edges of graphene and GNRs can be explained on the basis of the enhanced electron density edge effect.

1. Introduction

Graphene is a two-dimensional material consisting of a very large number of fused benzene rings [1,2]. Widths of graphene nanoribbons (GNRs) are much less than their lengths. As there is no band gap in graphene, it behaves as a semi-metal while GNRs behave as semiconductors since they have band gaps due to which they may be used to develop electronic devices [3]. It makes a detailed study of electronic structures and properties of GNRs very important. It is reported that graphene and GNRs have appreciably more reactive edges than their other parts [4–6]. Using sub-nanometer-resolved scanning tunneling microscopy, GNRs have been observed by Tao et al. to be associated with one-dimensional edge states, bright stripes running along the edges, and several other interesting properties [7]. Binding of atomic hydrogen to pyrene was found using density functional theory (DFT) by Rasmussen et al. [5] to be appreciably exothermic and strongly site-dependent, the edge carbon atoms being most reactive. These authors also showed employing a simple model that projected density of π-states can be used to predict the favored binding sites for hydrogen atoms [5]. In another study, Bonfanti et al. [8], using DFT, correlated wave functions and the notion of hypercoordination, showed the existence of a clear preference for adsorption of hydrogen atoms at the edge sites of small polycyclic aromatic hydrocarbons (PAHs). Electronic states of graphite ribbons with armchair and zigzag edges were studied by Fujita et al. [9] and it was found that the electronic states depend strikingly on the edge shape.

Kim et al. [6] have shown experimentally and using molecular dynamics simulation that peptides bind preferentially at the graphene edges. Umadevi and Sastry [10] studied interactions of certain small molecules, metal atoms and their ions with several PAHs, taken as models of graphene, using DFT. Feng et al. [11] have studied stacking of PAHs treated as finite size models of graphene multilayers using DFT. In a study by Peralta-Inga et al. [12], bond lengths of several PAHs taken as graphene models were optimized and MEP maps and average local ionization energies studied on the molecular surfaces [13,14]. In this work, MEP values above the carbon rings of the PAHs were found to be uniformly weakly negative, particularly in the central portions of the molecules indicating low reactivity of these regions while certain outer CC bonds were found to have considerable double bond character. Ab initio or density functional theoretic calculations have been performed extensively to study electronic and magnetic properties of GNRs including reactivity and it has been found that edges of GNRs are most reactive with respect to substitution of nitrogen atoms [15–18].

In a study that aims to shed light on the origin of edge effects in graphene and GNRs, an approach to investigate changes in properties of finite size fused benzene ring systems, i.e., PAHs, by varying their sizes and arrangements of rings systematically may be adopted. It would be interesting if any general trend is found in such a study as it may be qualitatively valid for graphene and GNRs also. Finite size PAHs are known for a long time to be interesting and important in different contexts, e.g., due to their occurrence in space [19], their roles as polluting materials [20] and as

* Corresponding author.
E-mail address: pcmishra_in@yahoo.com (P.C. Mishra).

0301-0104/$ - see front matter © 2012 Elsevier B.V. All rights reserved.
http://dx.doi.org/10.1016/j.chemphys.2012.04.005

carcinogens [21]. Molecular electronic structure theory can serve as a reliable tool in such a study as it can unravel the fundamental reasons for the different observed properties of graphene and GNRs. As electrons in graphene are known to be relativistic particles, ideally relativistic quantum theory should be used to study its electronic properties. However, since quantum relativistic effects in graphene are minute [22], application of non-relativistic formalisms of quantum theory to it may also yield quite useful information.

As electron density distribution is a fundamental aspect of materials, we have studied its general features in several PAHs. A novelty of the present work is that occurrence of enhanced electron density at the edges of a variety of PAHs has been shown to be a general edge effect. It can be used to explain the distinct edge properties observed in previous studies on PAHs, graphene and GNRs [3–7] at the fundamental level of electron density distribution. Though we have studied finite size PAHs as models of graphene and GNRs, an analysis of size dependence of the enhanced electron density edge effect suggests that this effect would be qualitatively valid for graphene and GNRs also. In a previous short communication, we showed occurrence of this edge effect in singlet states of certain other PAHs than those studied here [23]. In the present work, occurrence of this edge effect has been shown to exist in the ground states of several PAHs having different types of structures and sizes whether these have singlet or triplet ground state multiplicity.

2. Method of calculations

Several different functionals are available for use with DFT [24–27]. We employed the frequently used B3LYP functional which is thoroughly tested and found to yield results within acceptable error limits for ground states of organic systems including reactions [25–27]. The comparatively recently developed M06-2X functional [28] was also used to study a few cases so that the results obtained using it may be compared with those obtained employing the B3LYP functional. The 6-31G(d,p) Gaussian basis set was employed for the calculations. Continuous electronic charge density distribution was used to obtain molecular electrostatic potential (MEP) which, at a point r near a molecule (in a.u.), is defined as

$$V(\mathbf{r}) = \frac{\sum_A Z_A}{|\mathbf{R}_A - \mathbf{r}|} - \int \frac{\rho(\mathbf{r}')}{|\mathbf{r} - \mathbf{r}'|}\, d\mathbf{r}' \quad (1)$$

where Z_A stands for atomic number of atom A, R_A represents position vector of nucleus of atom A and $\rho(r')$ represents continuous electron density at the variable point r'. MEP is presented here in the form of features of iso-MEP surfaces. MEP, molecular electric field (MEF) and charge distributions have been widely used to explain molecular properties [29–41]. An advantage of using MEP or molecular electric field [31–39] is that while on one hand it reflects information about electron density distribution, on the other it also provides information about long range intermolecular interactions, e.g., hydrogen bonding and chemical reactivity towards electrophilic reactants. A close relationship between MEP and electron density is well established [42]. A correlation between carcinogenic activity and MEP features of certain carcinogens was shown long back [43].

Point charges located at the atomic sites in molecules provide an approximate but a convenient mode of quantitative representation of electron density distribution. Various methods are available to calculate point charges in molecules as discussed in the literature [33,35,36]. CHelpG and Merz–Singh–Kollman (MK) charges [44,45] are based on fitting to surface MEP obtained using continuous electron density distribution and describe molecular electrostatic properties, e.g., dipole moments, quite well [33,35,36]. Mulliken charges are obtained theoretically by partitioning of electron density distribution employing the Mulliken approximation [46]. CHelpG and MK charges have been shown to be more reliable to calculate molecular electrostatic properties than the Mulliken charges [33,35,36]. Therefore, CHelpG and MK charges [44,45] were analyzed for all the cases studied here. Mulliken charges [46] were also analyzed for three representative cases of different types for comparison of features revealed by the CHelpG and MK charges.

Continuous electron density distribution is presented as iso-density maps. We were interested in locating the regions of highest electron density in the various systems studied. The highest electron density values that could be located anywhere in the different systems were usually less than 0.32 electrons/Bohr^3. When electron density values less than 0.29 electrons/Bohr^3 were considered, the density got spread due to which locations of the regions of concentrated electron density could not be resolved. The electron density value of 0.295 electrons/Bohr^3 was found to be a value close to the highest one for which the regions of concentrated electron density could be resolved in the different cases. The lowest (most negative) MEP values which were somewhat different in the different cases were used to plot iso-MEP maps. If less negative MEP values than those used here were considered, the iso-MEP surfaces became extended due to which the most negative MEP regions could not be resolved. Further, if appreciably more negative MEP values than those used here were considered, the iso-MEP features located along the edges started disappearing. The MEP values used for iso-MEP plots were found to be close to the most negative values for which the edge effect could be resolved.

Features of iso-density maps may be compared with those revealed by the point charges. However, in making such a comparison, it is to be noted that while continuous iso-density maps show relative enhancement or depletion of density on bonds, particularly since we selected a high value of electron density as mentioned above, point charges by definition are located at the atomic sites. In spite of this difference, both the modes of representation of electron density distribution lead to broadly similar predictions of physical properties, e.g., surface MEP features. Spin density distributions were studied as iso-spin maps for those systems that have triplet ground states. All the calculations were carried out using the Windows version of the Gaussian 09 (G09W) suite of programs [47]. Molecular structures, iso-density, iso-MEP and iso-spin maps were visualized using the Windows version of the GaussView software (version 5.0) [48].

3. Results and discussion

We selected four types of PAHs for the present study: (i) Linear PAHs (linear polyacenes) having different numbers of condensed benzene rings arranged in a row and zig-zag edges. For these systems, we adopted the nomenclature 1R*m*, 1R standing for 1 row of condensed benzene rings and m standing for the number of rings in the row. Due to a single row of condensed benzene rings, linear PAHs may also be referred to as one-dimensional PAHs. (ii) PAHs that have n rows of condensed benzene rings, there being m rings in each row, and all the four edges are of zig-zag type. We adopted the nomenclature *n*R*m* (*n* = number of rows, *m* = number of rings in each row). In the present study, n lies between 2 and 5 while m lies between 2 and 10. (iii) PAHs having two zig-zag and two arm chair edges located on the opposite sides each. For these systems, we adopted the nomenclature ZnAn, where Z stands for zig-zag, A stands for arm chair and n is the number of rings on each of the zig-zag and arm chair edges. In the present study, $n = 2$, 3 and 4. (iv) In an *n*R*m* type system, 6 carbon atoms of a benzene ring located in the central part of the system were removed and the

valencies of the carbon atoms bonded to the removed carbon atoms got satisfied (passivated) by attaching hydrogens to them. This system has an inner arm chair edge while all of its outer edges are of zig-zag type. This system is denoted by *n*R*m*(A), A standing for the inner arm chair edge. For convenience of description, PAHs of the classes (ii), (iii) and (iv) would also be referred to as two-dimensional systems. Structures and adopted atomic numbering schemes for three systems, i.e., 1R5, 4R4 and Z3A3 are shown in Fig. 1(a)–(c), respectively while those for other two systems, i.e., 3R3 and Z4A4 are shown in Fig. S1(a) and (b) (Supporting information) respectively.

3.1. Ground state multiplicity

In previous studies, it was found that multiplicity (singlet or triplet) of the ground state of a polyacene depends on its size [49]. Therefore, we optimized molecular geometries and analyzed electron density distributions in the different PAHs considering both singlet and triplet multiplicities. The differences between the total energies obtained considering singlet and triplet multiplicities (ΔE_{S-T} = total energy of singlet – total energy of triplet) for the different systems studied are presented in Table 1. A negative ΔE_{S-T} implies singlet ground state while a positive ΔE_{S-T}

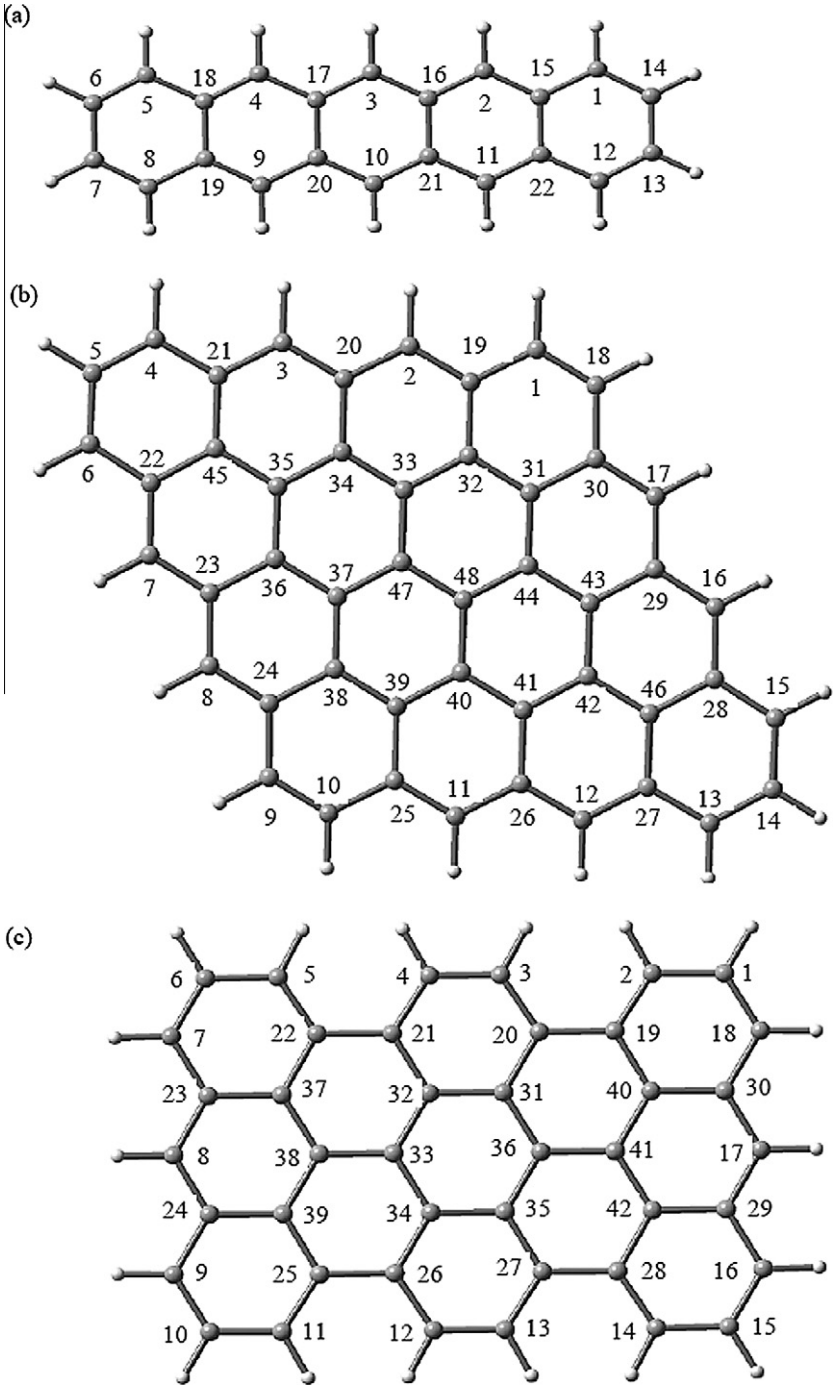

Fig. 1. Optimized structures and adopted atomic numbering schemes for three different systems: (a) 1R5 (singlet), (b) 4R4 (singlet) and (c) Z3A3 (triplet).

Table 1
Relative total energies (ΔE_{S-T} = energy of singlet – energy of triplet) (kcal/mol) obtained considering singlet and triplet multiplicities of different condensed benzene ring systems at the B3LYP/6-31G(d,p) level of theory.

Linear systems[a]		Two-dimensional systems	
System name	ΔE_{S-T}	System name	ΔE_{S-T}
1R1	−89.5	Zig-zag edges[b]	
1R2	−62.6	2R2	−48.5
1R3	−41.8	2R5	−10.1
1R4	−27.8	2R10	8.8
1R5	−17.9	3R3	−20.6
1R6	−10.9	3R5	−3.1
1R7	−5.7	3R10	14.1
1R8	−1.8	4R4	−3.3
1R9	1.19	4R5	2.7
1R10	3.4	4R10	21.4
1R15	6.8	5R10	27.4
1R20	6.2	Mixed edges[c]	
		Z2A2	−34.9
		Z3A3	0.7
		Z4A4	15.9
		5R5(A)	1.86

[a] Structures of some of these systems are shown in Figs. 2 and 3.
[b] Structures of some of these systems are shown in Figs. 4 and 6.
[c] Structures of some of these systems are shown in Figs. 5 and 7.

implies a triplet ground state. We find from the results presented in Table 1 that, broadly speaking, for smaller systems (e.g., 1R1 to 1R8 linear systems, 2R2, 2R5, 3R3, 3R5, 4R4 and Z2A2 two dimensional systems), the ground state multiplicity is singlet while for larger systems, the ground state multiplicity is triplet. Further, whether the singlet or triplet lies lower also depends on the way the benzene rings are arranged. For example, the ground state becomes triplet from singlet in going from 8 to 9 rings arranged linearly while it happens in going from 4R4 (16 rings) to 4R5 (20 rings) two dimensional systems. MEP and continuous electron density distribution maps and analyses of CHelpG and MK point charges are presented for the singlet or triplet multiplicity which corresponds to lower total energy.

3.2. Test of accuracy

It appears desirable to examine how accurately the B3LYP/6-31G(d,p) level of density functional theory predicts the structures of benzene and naphthalene, as PAHs are composed of benzene rings, and naphthalene is the first member of the PAH family. Fortunately, highly accurate geometries of these two molecules have recently become available from ultra high resolution laser spectroscopy [50]. The ground state CC and CH bond lengths of benzene optimized at the B3LYP/6-31G(d,p) level of theory were found to be 1.396 and 1.086 Å while the corresponding precisely determined experimental values [50] are 1.3969 and 1.0817 Å, respectively. The optimized ground state CC and CH bond lengths of naphthalene were found to be as follows (atomic numbering is given in Ref. [51]): C1C2 = 1.376, C2C3 = 1.417, C4C10 = 1.421, C1C9 = 1.434, C1H = 1.087 and C2H = 1.086 Å while the corresponding values obtained from the recent experimental study [50] are 1.3791, 1.4142, 1.4187, 1.4321, 1.0844 and 1.0829 Å, respectively. The optimized values of the bond angles [38] C1C9C10, C9C1H and C1C2H of naphthalene were found to be 118.8, 118.7 and 120.0 deg. while the corresponding experimental values [50] are 119.0, 118.7 and 120.1 deg. respectively. The good agreement between the optimized and experimental geometrical parameters shows that the B3LYP/6-31G(d,p) level of theory is quite reliable to study ground state structures and properties of PAHs.

3.3. Charge distribution and MEP maps of linear PAHs

Net CHelpG charge distribution in the linear five benzene ring system (1R5), taken as an example of linear systems with singlet multiplicity (Table 1), is given (in the unit of magnitude of electronic charge) in Fig. 2(a). In this and all other systems studied by us, all the carbon atoms to which hydrogen atoms are attached (denoted as C_H type carbon atoms) are associated with negative net charges while the carbon atoms directly bonded to the C_H type carbon atoms (denoted as C_C type carbon atoms) are associated with net positive charges. In benzene, there is no C_C type carbon atom, and at the B3LYP/6-31G(d,p) level of theory, each C_H type carbon atom is associated with a net CHelpG charge equal to −0.084 while the corresponding MK charge is −0.117.

In the linear five ring system (Fig. 2(a)), with singlet multiplicity (Table 1), the sum of net CHelpG charges at all the C_H type carbon atoms (atoms 1-14 in Fig. 1(a)) is −2.952 (average −0.211 per atom) while the sum of the net CHelpG charges at all the Cc type carbon atoms (atoms 15–22 in Fig. 1(a)) is 1.356 (average 0.170 per atom). The sum of net CHelpG charges at all the carbon atoms including those of both C_H and C_C types (atoms 1–22 in Fig. 1(a)) is −1.596 (average −0.073 per atom). The corresponding average MK and Mulliken charges per carbon atom are −0.085 and −0.054 respectively. In the 3, 10 and 20 ring linear polyacenes, the sums of charges at C_H type carbons were found to be –1.838 (average −0.184 per atom), −6.056 (average −0.252 per atom) and −11.988 (average −0.272 per atom) respectively. In these systems, the sums of net charges at all the carbon atoms including those of both C_H and C_C types were found to be −1.094 (average −0.078 per atom), −2.945 (average −0.070 per atom) and −5.592 (average −0.068 per atom) respectively. The corresponding average MK charges per atom including the atoms of both the C_H and C_C types were found to be −0.093, −0.078 and −0.074 respectively. Thus we find that the MK charges are somewhat larger in magnitude than the CHelpG charges but the difference between the two diminishes as we go from smaller to larger linear systems. Further, both the CHelpG and MK charges vary in a similar way in going from one system to another.

The continuous iso-density map for the electron density value 0.295 electrons/Bohr^3 for the five ring linear system is shown in Fig. 2(b). In this figure, it is noted that electron density is comparatively enhanced at many CC bonds located at the edges along the length while it is comparatively depleted on the CC bonds located between the rings and on the two end CC bonds that are not shared by other benzene rings. However, the end C_H type carbon atoms (atoms numbers 6, 7, 13 and 14 in Fig. 1(a)) are associated with net negative charges. Thus, on the whole, we find that the edges of linear polyacences are associated with net negative charges.

In the linear nine ring system (1R9) having triplet ground state (Table 1) taken as an example of linear systems with triplet multiplicity, the sum of net CHelpG charges at all the C_H type carbon atoms was found to be −5.392 (average −0.245 per atom) while the sum of the net charges at all the C_C type carbon atoms was found to be 2.724 (average 0.170 per atom). The sum of net CHelpG charges at all the carbon atoms including those of both C_H and C_C types in the 1R9 system was found to be −2.668 (average −0.070 per atom). The corresponding average MK charge per atom in this case was found to be −0.078. Calculations of charges were also performed for this system considering singlet multiplicity, and similar results as those obtained with triplet multiplicity were found.

Iso-MEP maps for the certain linear systems, i.e., 1Rn, n = 1, 2, 3, 5, 10, 20 obtained using continuous electron density are presented in Fig. 3. In each of these cases, for drawing the iso-MEP maps, the lower total energy multiplicity (singlet or triplet) was considered (Table 1). In each of these and other MEP maps presented in this work, the red and yellow regions correspond to the same MEP

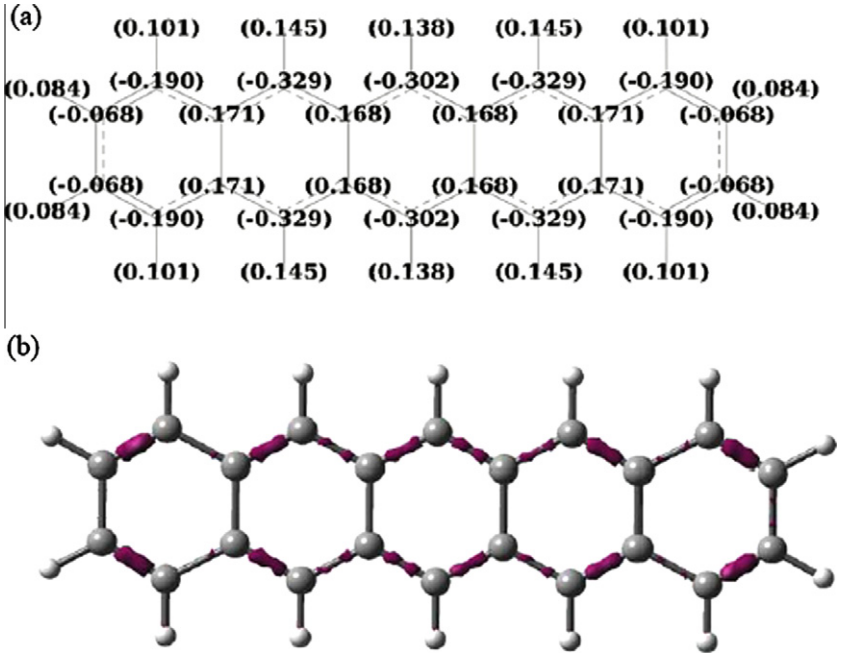

Fig. 2. Electron density distribution in a system having a row of five benzene rings and zig-zag edges (1R5) (singlet multiplicity). (a) Net CHelpG charges at the atomic sites, (b) continuous iso-density map for electron density 0.295 electrons/Bohr^3.

magnitude but with opposite signs. Further, the negative MEP value corresponding to the red patches is given near each map (Fig. 3). In benzene, the minimum MEP value is located in a circular region above and below the ring at a distance of about 1.65 Å, as has been discussed earlier [52]. The iso-MEP maps of all linear polyacenes where minimum MEP values are found above and below the molecular planes show that negative iso-MEP features are located along the edges (Fig. 3). The end portions along the lengths of all the linear systems studied here are associated with somewhat extended negative iso-MEP regions (Fig. 3) because four carbon atoms in succession on each side in these systems are associated with net negative charges, and this sort of environment is not present in any other region in any case (Fig. 2(a)).

Iso-MEP distribution, total electron density distribution and net CHelpG charges for the linear system with three benzene rings (1R3) obtained at the B3LYP/6-31G(d,p) and M06-2X/6-31G(d,p) levels of theory are presented in Fig. S2 (Supporting information). We find that the results obtained using the B3LYP and M06-2X functionals are very similar. Thus the M06-2X/6-31G(d,p) level calculations also show that electron density and negative MEP are noticeably enhanced along the edges of linear systems (Fig. S2).

3.4. Electron density distribution in two-dimensional PAHs with zig-zag edges

The notations of C_H and C_C type carbon atoms defined for linear systems would also be used for two dimensional systems. The CHelpG net charge distribution in the 4R4 system, taken as an example of two-dimensional systems with zig-zag edges, is presented in Fig. 4. The ground state multiplicity of this system is singlet as the triplet multiplicity corresponds to 3.3 kcal/mol higher energy than that of the singlet (Table 1). Obviously, in two-dimensional systems, beside those of C_H and C_C type atoms located along the edges, we also have other carbon atoms that are located away from the edges. We get the following information from an analysis of the net CHelpG, MK and Mulliken charges in the 4R4 system (Fig. 4): (i) The sum of CHelpG charges on the C_H type atoms located on the edges (atoms 1–18 in Fig. 1(b)) is −4.456 (average −0.248 per atom) while the sum of charges on the corresponding C_C type carbon atoms (atoms 19–30 in Fig. 1(b)) is 2.700 (average 0.225 per atom). The total of these two sums of net charges on atoms located along the edges of the 4R4 system (atoms 1–30 in Fig. 1(b)) (set 1) is −1.756, the average CHelpG charge per carbon atom being −0.058 while the corresponding average MK and Mulliken charges are −0.079 and −0.048 respectively. (ii) The sum of net charges on the second inner line of carbon atoms (atoms 31–46 in Fig. 1(b)) (set 2) and two remaining carbon atoms (atoms 45, 46 in Fig. 1(b)) not included in any of the sets 1 and 2 is −0.428, the average CHelpG charge per carbon atom being −0.027 while the corresponding average MK and Mulliken charges are −0.004 and −0.007 respectively (Fig. 4(a)). (iii) The sum of net charges on the two innermost carbon atoms (atoms 47, 48 in Fig. 1(b)) (set 3) of the 4R4 system, not included in any of the sets 1 and 2 is −0.004, the average CHelpG charge per carbon being −0.002 while the corresponding MK and Mulliken charges are −0.003 and 0.012 respectively (Fig. 4(a)). Thus we find that variations of CHelpG, MK and Mulliken charges in going from the outer to inner regions of the 4R4 system are qualitatively similar.

This analysis of net charges (Fig. 4(a)) shows that there is an enhancement of electron density along the edges of the 4R4 system and electron density per carbon atom decreases as we go from the edges towards the inner regions of the same. Further, we find that though variations of CHelpG and MK charges in going from the edges of the 4R4 system to the inner regions are qualitatively similar, variation of the latter charges is more rapid than that of the former. The continuous iso-density distribution for the 4R4 system presented in Fig. 4(b) also shows that electron density is enhanced along its edges. Electron density distributions in several other two-dimensional systems with zig-zag edges studied by us, e.g., 2R2, 2R5, 2R10, 3R5, 3R10, 4R5, 4R10 and 5R10 (not presented here) also show that electron density is enhanced at their edges whether the ground state multiplicity is singlet or triplet.

Net charges, iso-density maps and iso-MEP maps for the 3R3 two dimensional system obtained at the B3LYP/6-31G(d,p) and M06-2X/6-31G(d,p) levels of density functional theory are presented in Figs. S3 and S4, respectively (Supporting information).

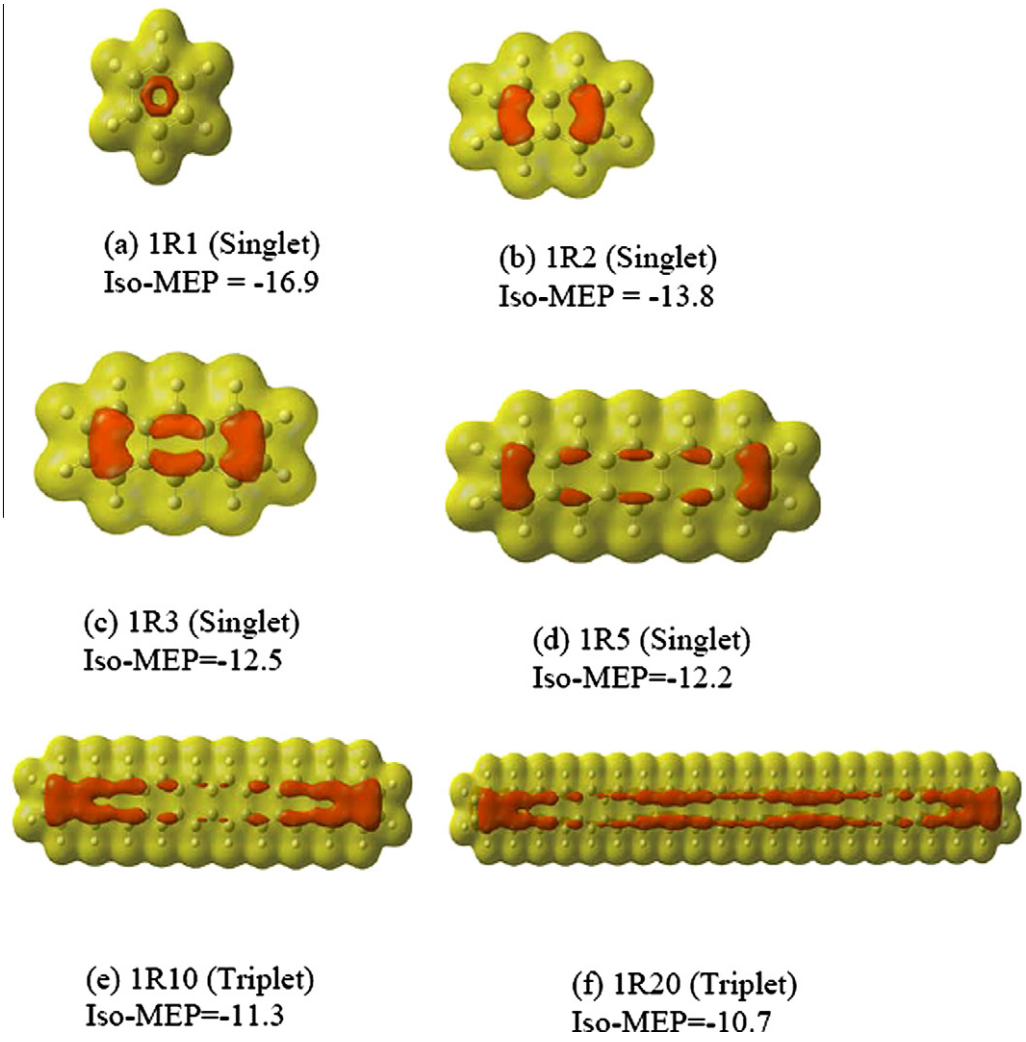

Fig. 3. Iso-MEP maps (kcal/mol) obtained using continuous electron density for (a) 1R1 (benzene), (b) 1R2, (c) 1R3, (d) 1R5, (e) 1R10 and (f) 1R20 linear systems with zig-zag edges. The red and yellow regions correspond to the same MEP magnitude but with opposite signs. The negative iso-MEP values (red regions) considered for the different plots are given near the maps. Singlet or triplet multiplicity that corresponds to lower energy is specified. (For interpretation of the references to colour in this figure legend, the reader is referred to the web version of this article.)

A comparison of the corresponding results presented in these figures shows that both the B3LYP and M06-2X functionals yield similar results showing enhancement of edge electron density.

3.5. Electron density distribution in two-dimensional PAHs with mixed edges

In the two dimensional system named Z3A3, the total energy with triplet multiplicity lies lower than that with singlet multiplicity by 0.7 kcal/mol (Table 1). Therefore, in this case the charge analysis is performed for triplet multiplicity. This system has two zig-zag and two arm chair edges, there being three benzene rings on each of the edges and thirteen benzene rings in total (Fig. 5(a)). The net CHelpG charge distribution in the Z3A3 system (Fig. 5(a)) reveals the following information: (i) The sum of net CHelpG charges on the C_H type carbon atoms of the two arm chair edges (atoms 1–6, 10–15 in Fig. 1(c)) (set 1) is −1.360 (average −0.113 per atom) while the sum of net charges on the C_C type carbon atoms of the two arm chair edges (atoms 19–22, 25–28 in Fig. 1(c)) (set 2) is 0.288 (average 0.036 per atom). Therefore, the sum of net CHelpG charges on all the carbon atoms of the two arm chair edges (set 1 + set 2) is −1.072, the average CHelpG charge per carbon atom being −0.054 while the corresponding average MK and Mulliken charges are −0.078 and −0.059 respectively. (ii) In the same system, the sum of net CHelpG charges on the C_H type carbon atoms of the two zig-zag edges (atoms 7–9, 16–18 in Fig. 1(c)) (set 3) is −1.550 (average −0.258 per atom) while the sum of net charges on the C_C type carbon atoms of the two zig-zag edges (atoms 23, 24, 29, 30 in Fig. 1(c)) (set 4) is 0.852 (average 0.213 per atom). The sum of net CHelpG charges on all the carbon atoms of the two zig-zag edges (set 3 + set 4) is −0.698, the average CHelpG charge per carbon atom being −0.069 while the corresponding average MK and Mulliken charges are −0.081 and −0.054 respectively. (iii) The sum of net CHelpG charges on all the carbon atoms considered above including those of the two zig-zag and two arm chair edges (sets 1 to 4) is −1.770, the average CHelpG charge per carbon atom being −0.059 while the corresponding average MK and Mulliken charges are −0.080 and −0.057 respectively. (iv) The total net CHelpG charges on all the inner carbon atoms not included in the above four sets (atoms 31–42 in Fig. 1(c)) is −0.102, the average CHelpG charge per carbon atom being −0.008 while the corresponding average MK and Mulliken charges are 0.003 and 0.014 respectively. The charges calculated for the Z3A3 system considering singlet multiplicity were found to be similar to those obtained considering triplet multiplicity.

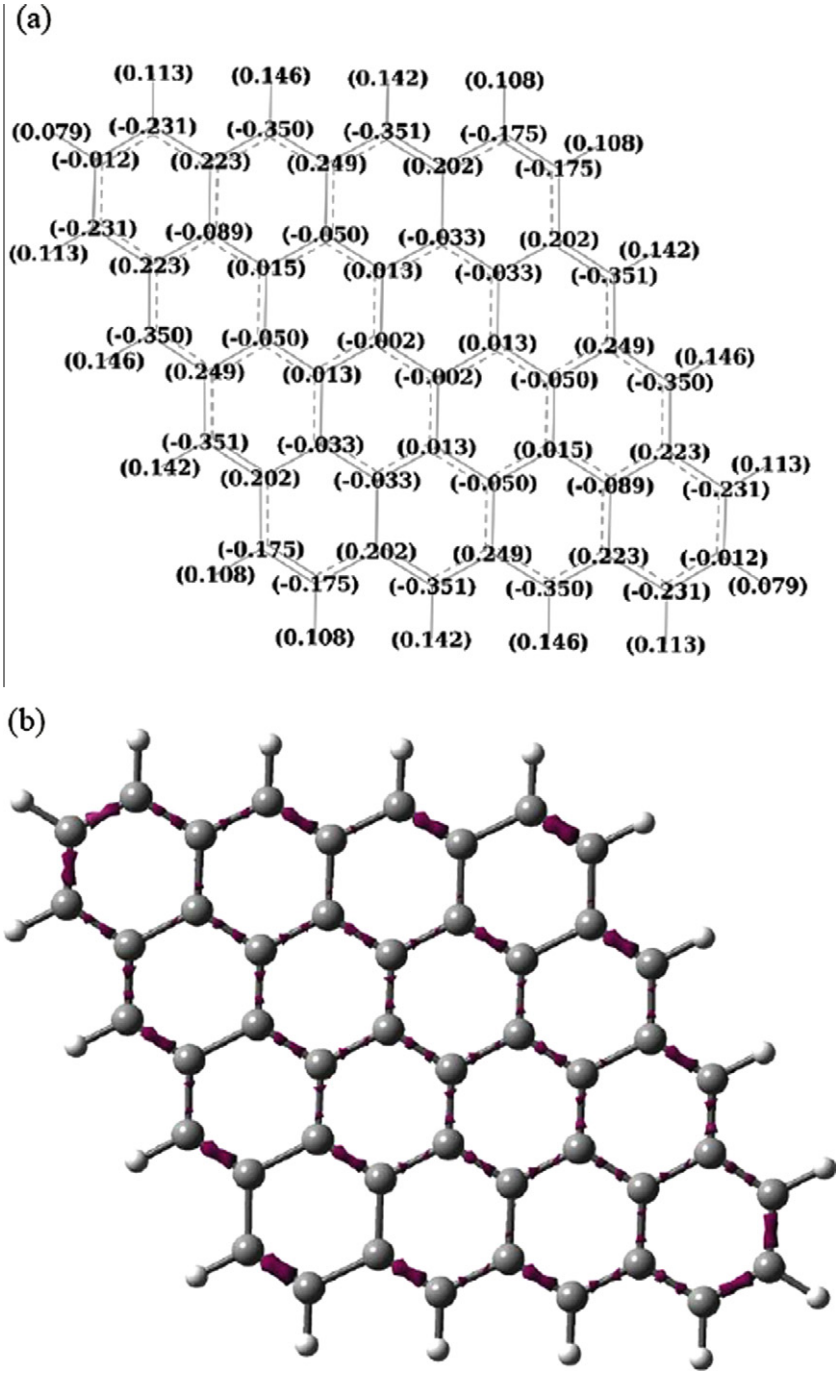

Fig. 4. Results obtained for the 4R4 system at the B3LYP/6-31G(d,p) level of theory (singlet multiplicity). (a) ChelpG charges, and (b) iso-density map for electron density value 0.295 electrons/Bohr^3.

Thus we find that the carbon atoms located at the edges of the Z3A3 system with tripet multiplicity are on the average associated with more negative charges than those in the inner parts of the same. Further, though, qualitatively speaking, both the CHelpG and MK charges reveal similar variations in going from the edges to the inner regions of the Z3A3 system, quantitative variation in the latter charges is more rapid than that in the former. Also, in going from the outer to the inner regions of the Z3A3 system, Mulliken charges are found to vary qualitatively in a similar manner as the CHelpG and MK charges. The continuous electron density distribution in the Z3A3 system with triplet multiplicity presented in Fig. 5(b) also shows that more electron density is associated with its edges than with the inner parts of the same.

Distributions of net CHelpG charges in a two-dimensional system that has two zig-zag and two arm chair edges and twenty five benzene rings in total (named as Z4A4) is presented as a part of the Supporting information (Fig. S5(a)) where an analysis of these charges is also given. This analysis reveals that, on the average, more negative charges are associated with the carbon atoms located at the edges of the system than those with the inner parts of the same. The continuous electron density distribution in the Z4A4 system presented in Fig. S5(b) (Supporting information) also

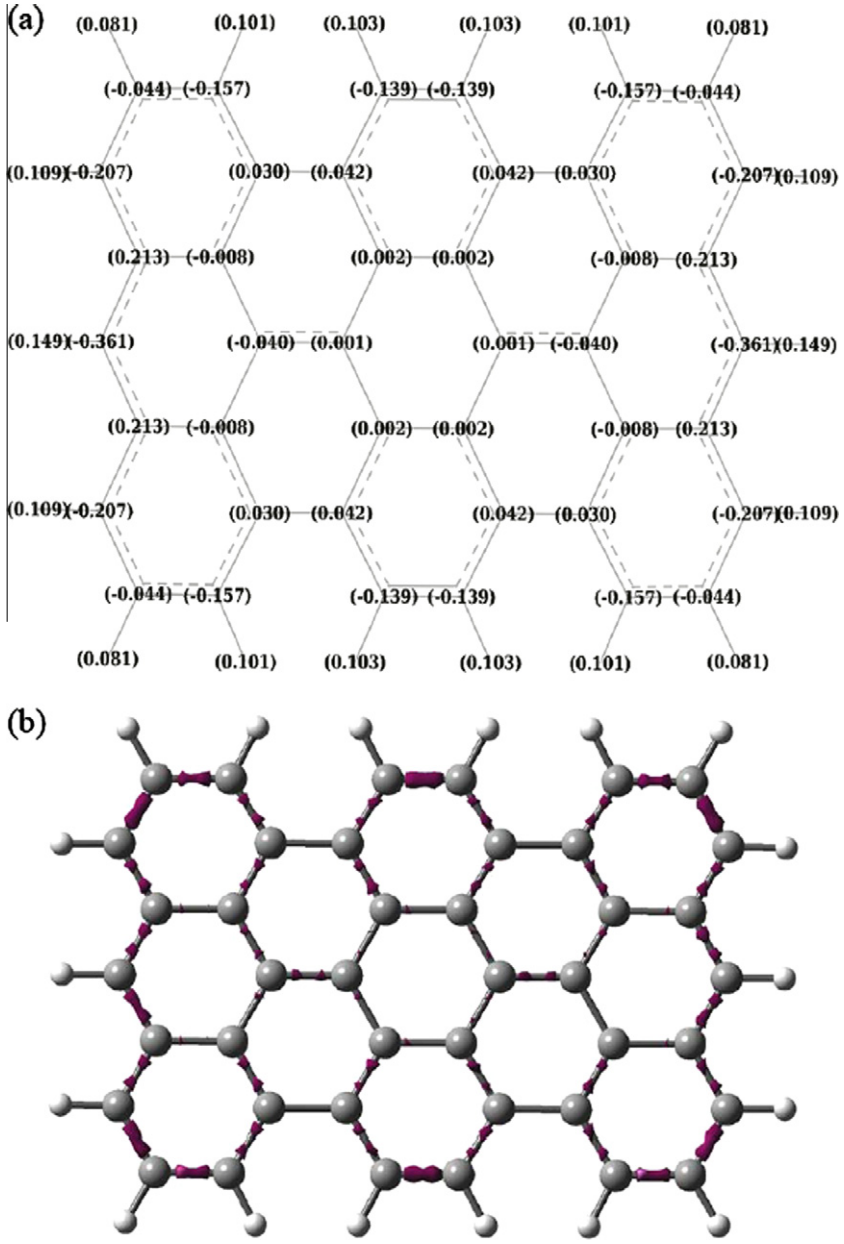

Fig. 5. Electron density distribution in the triplet Z3A3 system having two zig-zag and two arm chair edges, three rings on each edge and 13 benzene rings in total (triplet multiplicity). (a) Net CHelpG charges, (b) Continuous iso-density map for electron density 0.295 electrons/Bohr^3.

shows that more electron density is associated with its edges than with its inner parts.

3.6. Iso-MEP maps of two-dimensional PAHs

Iso-MEP maps of two-dimensional 2R5, 3R5, 4R4, 4R5, 2R10, 3R10, 4R10 and 5R10 condensed benzene ring systems with zig-zag edges obtained at the B3LYP/6-31G(d,p) level of theory are presented in Fig. 6. In each of these cases, the lower total energy multiplicity (singlet or triplet) was considered for drawing the iso-MEP maps. The corresponding multiplicity and iso-MEP values are given near the maps (Fig. 6(a)–(h)). These maps show that the edges of the different two-dimensional condensed benzene ring systems, in comparison to the corresponding inner regions, are associated with enhanced negative MEP values and hence enhanced electron density. Similar features were also found in the MEP maps of all other two-dimensional systems studied by us but not reported here.

Iso-MEP maps of three two-dimensional systems having two zig-zag and two arm chair edges each are presented in Fig. 7. There are two (Z2A2), three (Z3A3) and four (Z4A4) benzene rings on each of the zig-zag and arm chair edges in these systems. While in the Z2A2 system, the lower energy multiplicity is singlet, in the latter two, it is triplet (Table 1). These iso-MEP maps confirm existence of the effect of enhanced electron density along the edges discussed above. A difference may be noted between the iso-MEP features at the zig-zag and arm chair edges. That is, the iso-MEP regions at the arm chair edges are somewhat more extended than those at the zig-zag edges (Fig. 7). This difference arises because of the fact that while single C_H and C_C type carbon atoms occur alternately at the zig-zag edges and are associated with net negative and positive charges respectively, the corresponding two types of carbon atoms occur at the arm chair edges in pairs and are also

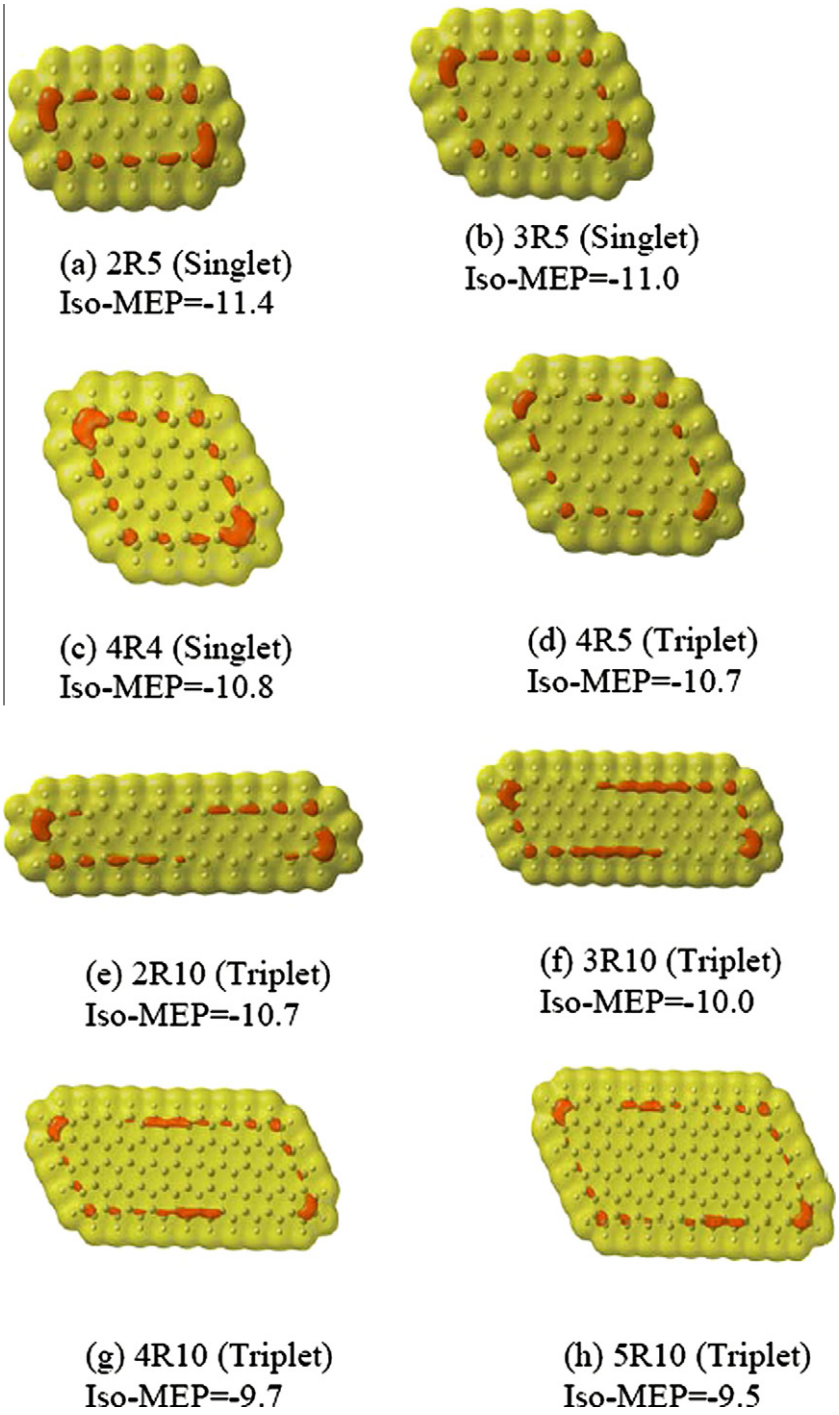

Fig. 6. Iso-MEP maps (kcal/mol) obtained using continuous electron density for (a) 2R5, (b) 3R5, (c) 4R5, (d) 5R5, (e) 2R10, (f) 3R10, (g) 4R10 and (h) 5R10 condensed benzene ring systems with zig-zag edges. The red and yellow regions correspond to the same MEP magnitude but with opposite signs. The negative iso-MEP values (red regions) considered for the different plots are given near the maps. Singlet or triplet multiplicity that corresponds to lower energy is specified. The corresponding multiplicities are also given. (For interpretation of the references to colour in this figure legend, the reader is referred to the web version of this article.)

associated with net negative and positive charges respectively. Thus the localization of negative and positive charges is more pronounced at the arm chair edges than at the zig-zag edges. The bay regions of carcinogenic PAHs are structurally similar to the arm chair regions of the arm chair edges [32,53,54]. The bay regions of PAHs are known to be more reactive than their other regions from the point of view of involvement of these molecules in carcinogenesis [32,43,53,54]. This fact may be broadly correlated with the somewhat more extended iso-MEP regions on the arm chair edges than those on the zig-zag edges. However, different arrangements of benzene rings in the various bay region PAHs provide them different reactivities [32,43,53,54] as expected.

The iso-density and iso-MEP maps of a two-dimensional system named as 5R5(A) which was obtained from a 5R5 system with zig-zag edges by removing the central benzene ring and getting valencies of carbon atoms which were bonded to the removed carbon atoms satisfied by attaching hydrogens to them (hydrogen passivated edges), are shown in Fig. 8(a,b) respectively. In this case, the

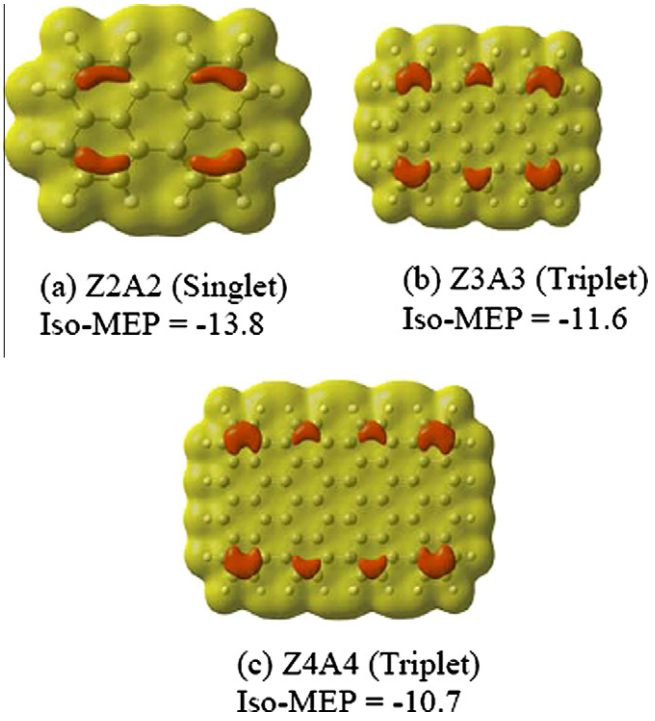

Fig. 7. Iso-MEP maps (kcal/mol) for systems with two zig-zag and two arm chair edges having n rings on each edge (ZnAn) ($n = 2, 3, 4$) obtained using continuous electron density. The red and yellow regions correspond to the same MEP magnitude but with opposite signs. The negative iso-MEP values (red regions) considered for the different plots are given near the maps. Singlet or triplet multiplicity that corresponds to lower energy is also specified. (For interpretation of the references to colour in this figure legend, the reader is referred to the web version of this article.)

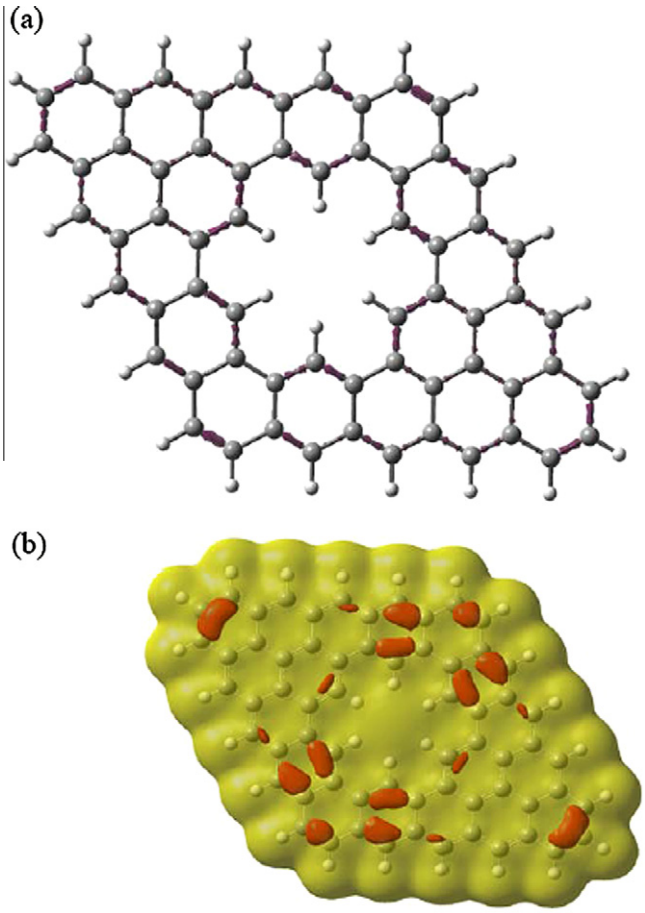

Fig. 8. 5R5(A) system prepared from the 5R5 system by removing its central benzene ring and hydrogen passivating the inner edges so created. (a) Continuous iso-density map for electron density 0.295 electrons/Bohr^3, (b) Iso-MEP map for the MEP value −10.7 kcal/mol (red regions). Multiplicity of the system considered was triplet. The red and yellow regions correspond to the same MEP magnitude but with opposite signs. (For interpretation of the references to colour in this figure legend, the reader is referred to the web version of this article.)

singlet multiplicity corresponds to 1.86 kcal/mol higher energy than the triplet, and thus the ground state is a triplet (Table 1). An interesting property revealed by this system is that electron density is localized at both of its outer (zig-zag) and inner (arm chair) edges (Fig. 8(a,b)). Consideration of singlet multiplicity revealed an iso-MEP distribution pattern that had only minor differences from the one found with triplet multiplicity (Fig. 8(b)). The results discussed above confirm that enhanced electron density is a general edge effect in PAHs whether the ground state multiplicity of the system under study is singlet or triplet.

3.7. Comparison of singlet and triplet state iso-MEP maps

Iso-MEP maps were found to be qualitatively similar, showing occurrence of the enhanced electron density edge effect, whether the ground state multiplicity of the system considered was singlet or triplet. However, certain minute differences between the features of iso-MEP maps were found for singlet and triplet multiplicities. Thus the MEP patches located along the edges in the iso-MEP maps of systems with triplet multiplicity presented in Fig. 3(e), (f) and 6(d)–(h) are not as uniform as those in the systems with singlet multiplicity (Fig. 3(a)–(d) and 6(a)–(c)). In the iso-MEP map of Fig. 3(e), along each of the two long edges, the MEP magnitudes are appreciably less in the middle region, conforming to structural symmetry, than those elsewhere. In the iso-MEP map of Fig. 3(f), along each of the two longer edges, the MEP magnitudes are appreciably less in three different regions than those elsewhere. In the iso-MEP maps of Fig. 6(d)–(h), in each case and along each of the two longer edges, the MEP magnitudes are appreciably less in one region than those elsewhere. A comparison of the MEP features of the 5R5(A) system with triplet multiplicity shown in Fig. 8(b) with those of the same system with singlet multiplicity (not shown) revealed that the iso-MEP patches along the edges were much more uniform in the latter case than those in the former. In the cases where MEP patches are invisible in specific regions, these would appear if MEP magnitudes are appropriately reduced. However, on doing so, not only all the parts of the edges but also some of the central parts of the molecules would get covered by MEP patches, which may mask appearance of the edge effect. The features of iso-MEP maps of systems with singlet multiplicity found in the present study are qualitatively similar to those reported for other systems earlier for the same multiplicity [23]. However, the results discussed above show that in systems with triplet multiplicity, electron localization is not as uniform as in systems with singlet multiplicity. Instead, in systems with triplet multiplicity, electron localization along the edges is more in certain regions than elsewhere.

3.8. Iso-spin density maps

Spin density distributions in triplet states of the systems would correspond to their magnetic properties [9]. Both positive and negative spin density values occur and correspond to ferromagnetic and antiferromagnetic spin alignments respectively [55]. Iso-spin

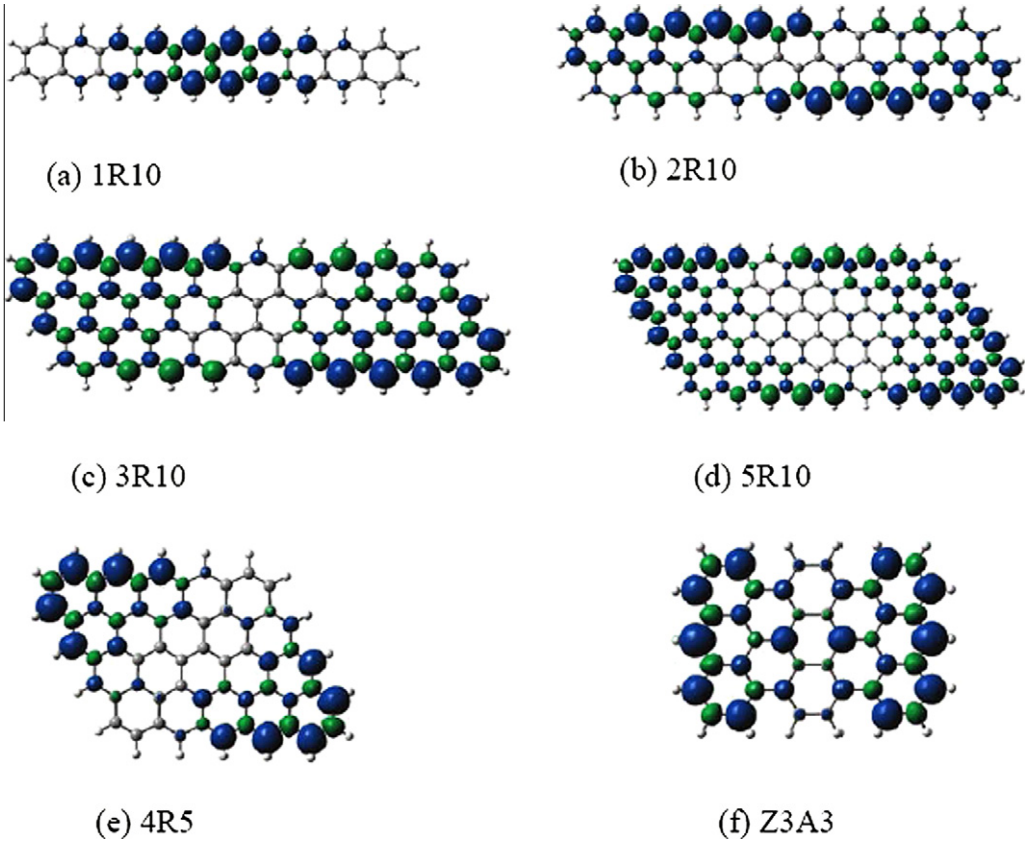

Fig. 9. Iso-spin density maps for the spin density value of 0.002 electrons/Bohr^3 in the triplet ground states of (a) 1R10, (b) 2R10, (c) 3R10, (d) 5R10 (e) 4R5 and (f) Z3A3 systems. Blue color represents positive spin density while green color represents negative spin density, the magnitude being the same for both the colors. (For interpretation of the references to colour in this figure legend, the reader is referred to the web version of this article.)

density maps in the triplet ground states of 1R10, 2R10, 3R10, 5R10, 4R5 and Z3A3 condensed benzene ring systems for the spin density value 0.002 electrons/Bohr^3 are presented in Fig. 9(a)–(f), respectively. As these maps show, broadly speaking, edge effect occurs in spin density distribution also. However, it is found that spin density is more localized in certain regions than elsewhere along the edges. Thus it is noted that in Fig. 9(b)–(e), spin densities, particularly positive ones (represented by blue color), are more localized at the portions of the edges located near the ends of the longer diagonals of the systems than those near the ends of the shorter diagonals. In the Z3A3 system (Fig. 9(f)), the zig-zag edges are associated with more positive or negative spin density than the arm chair ones.

3.9. Relevance to graphene and GNRs

An analysis of dependence of edge electron density on size of PAHs is desirable. Average net CHelpG and MK charges at the carbon atoms of both C_H and C_C types considered together along with total numbers of these two types of carbon atoms for linear and two-dimensional systems are collected in Table 2. For linear systems, considering the appropriate (singlet or triplet) multiplicities (Table 2), it is found that as the total number of carbon atoms (N_C) varies from 6 to 82 (N_C=$4N_B + 2$, where N_B is the number of benzene rings), the average net CHelpG charge varies from −0.084 to −0.067 while the corresponding average MK charge varies from −0.117 to −0.074. Further, the variation of both the average CHelpG and MK charges becomes appreciably slower when the linear system size increases, say beyond 7 rings (30 carbon atoms). For two-dimensional systems of *n*R*m* type (*n*, *m* = 2–4 with zig-zag edges), when the total number of carbon atoms of C_H and C_C types varies from 14 to 30, the average net CHelpG charge varies from −0.070 to −0.058 while the corresponding average net MK charge varies from −0.095 to −0.079. Further, both the CHelpG and MK charges are only slightly different between the larger two (3R3 and 4R4) systems. For two-dimensional ZnAn type systems (n = 2–4) having mixed types of edges, when the number of carbon atoms varies from 18 to 42, the average net CHelpG charge varies from −0.068 to −0.056 while the corresponding average net MK charge varies from −0.092 to −0.073. In the two-dimensional systems, variations of average net CHelpG and MK charges with system size become very slow near the largest sizes considered here. Though the system sizes considered here are quite limited, the results obtained seem to suggest that in going from small size PAHs to appreciably larger ones, the edge carbon atoms on the average would continue to be associated with appreciably negative net charges. Therefore, it appears that the edges of PAHs would, in general, be reactive towards electrophiles.

It has been experimentally observed that the edges of graphene and GNRs are appreciably more reactive than the bulk [4–6]. In particular, it has been found that peptides bind at the edges of graphene preferentially [6]. Indications for existence of the effect of enhanced edge electron density have also been found in electronic transport studies. Thus Xu et al. [56] investigated room-temperature electronic transport in graphene and GNRs and showed that the transport in GNRs lies in a localization regime. In view of the various experimental observations [4–6,9,56], it appears that the enhanced electron density edge effect found in PAHs would be relevant to graphene and GNRs also. However, quantification of the edge effect on electron density distribution in graphene and GNRs and role of relativistic effects in this regard remain to be investigated.

Table 2
Average net CHelpG charges at the carbon atoms located at the edges including those of both C_H and C_C types in different condensed benzene ring systems obtained at the B3LYP/6-31G(d,p) level of theory. Number of carbon atoms stands for the sum of numbers of carbon atoms of both C_H and C_C types.

Linear systems[a]		Two-dimensional systems	
System name (no. of carbon atoms)[b]	Average net charge per carbon atom[c]	Type of edge, System name (no. of carbon atoms)[b]	Average net charge per carbon atom[c]
1R1 (6)S	−0.084 [−0.117]	Zig-zag edges[d]	
1R2 (10)S	−0.080 [−0.102]	2R2 (14)S	−0.070 [−0.095]
1R3 (14)S	−0.078 [−0.093]	3R3 (22)S	−0.059 [−0.081]
1R4 (18)S	−0.074 [−0.088]	4R4 (30)S	−0.058 [−0.079]
1R5 (22)S	−0.073 [−0.085]		
1R6 (26)S	−0.072 [−0.082]	Mixed edges[e]	
1R7 (30)S	−0.071 [−0.081]	Z2A2 (18)S	−0.068 [−0.092]
1R8 (34)S	−0.071 [−0.079]	Z3A3 (30)T	−0.059 [−0.080]
1R9 (38)T	−0.070 [−0.078]	Z4A4 (42)T	−0.056 [−0.073]
1R10 (42)T	−0.069 [−0.078]		
1R15 (62)T	−0.069 [−0.075]		
1R20 (82)T	−0.067 [−0.074]		

[a] Structures of some of these systems are shown in Figs. 2 and 3.
[b] The letter S indicates that singlet multiplicity corresponds to lower total energy than triplet multiplicity while the letter T indicates the reverse situation.
[c] MK charges are given in brackets.
[d] Structures of some of these systems are shown in Figs. 4 and 6.
[e] Structures of some of these systems are shown in Figs. 5 and 7.

Graphene is known to be a good electrical conductor [57]. The present results indicate that if GNRs are arranged in parallel, they can carry high electrical current. Thus high electrical current carrying devices may be developed using GNRs. Small width GNRs, due to the enhanced electron density edge effect, may be more suited than graphene sheets in various electronic applications [58].

4. Conclusion

We arrive at the following conclusions from the present study:

(1) Electron density is appreciably enhanced at the edges of PAHs. This edge effect occurs even at the hydrogen passivated internal edges created by removing carbon atoms of benzene rings from the inner parts of PAHs.
(2) The enhanced electron density edge effect occurs whether the ground state multiplicity of the system under study is singlet or triplet. However, when the multiplicity is singlet, the enhancement of electron density along the edges is more uniform than when the multiplicity is triplet. It indicates that electrons are more localized along the edges in specific regions when the multiplicity is triplet than when it is singlet.
(3) On the basis of the enhanced electron density edge effect and iso-MEP features, it appears that edges of PAHs in general would be more reactive towards electrophiles than their other parts. Further, this effect also shows that the arm chair edges would be more reactive towards electrophiles than the zig-zag edges.
(4) Spin densities in PAHs with triplet ground state multiplicity are also enhanced at the edges in comparison to those in their other parts. However, these are more localized in certain portions of the edges than elsewhere on the same.
(5) The edges of graphene and GNRs have been experimentally found to be more reactive than their other parts. These experimental observations can be qualitatively explained by assuming validity of the enhanced electron density edge effect found in PAHs to graphene and GNRs also. However, the possible role of relativistic effects present in graphene and GNRs in this regard remains to be investigated.

Acknowledgements

The authors are thankful to the University Grants Commission (New Delhi) and the Council of Scientific and Industrial Research (New Delhi) for financial support.

Appendix A. Supplementary data

Supplementary data associated with this article can be found, in the online version, at http://dx.doi.org/10.1016/j.chemphys.2012.04.005.

References

[1] A.K. Geim, K.S. Novoselov, Nature 6 (2007) 183.
[2] C.N.R. Rao, A.K. Sood, J. Phys. Chem. Lett. 1 (2010) 572.
[3] M. Acik, Y.J. Chabal, Jpn. J. Appl. Phys. 50 (2011) 070101.
[4] R. Sharma, J.H. Baik, C.J. Perera, M.S. Strano, Nano Lett. 10 (2010) 398.
[5] J.A. Rasmussen, G. Henkelman, B. Hammer, J. Chem. Phys. 134 (2011) 164703.
[6] S.N. Kim, Z. Kuang, J.M. Slocik, S.E. Jones, Y. Cui, B.L. Farmer, M.C. McAlpine, R.R. Naik, J. Am. Chem. Soc. 133 (2011) 14480.
[7] C. Tao, L. Jiao, O.V. Yazyev, Y.-C. Chen, J. Feng, X. Zhang, R.B. Capaz, J.M. Tour, A. Zettl, S.G. Louie, H. Dai, M.F. Crommie, Nat. Phys. 7 (2011) 616.
[8] M. Bonfanti, S. Casolo, G.F. Tantardini, A. Ponti, R. Martinazzo, J. Chem. Phys. 135 (2011) 164701.
[9] M. Fujita, K. Wakabayashi, K. Nakada, K. Kusakabe, J. Phys. Soc. Jpn. 65 (1996) 1920.
[10] D. Umadevi, G. Narahari Sastry, J. Phys. Chem. C 115 (2011) 9656.
[11] C. Feng, C.S. Lin, W. Fan, R.Q. Zhang, M.A. Van Hove, J. Chem. Phys. 131 (2009) 194702.
[12] Z. Peralta-Inga, J.S. Murray, M.E. Grice, S. Boyd, C.J. O'Connor, P. Politzer, J. Mol. Struct. (Theochem) 549 (2001) 147.
[13] P. Politzer, J.S. Murray, F.A. Bulat, J. Mol. Model. 16 (2010) 1731.
[14] J.S. Murray, F. Abu-Awwad, P. Politzer, J. Mol. Struct. (Theochem) 501–502 (2000) 241.
[15] Y. Li, Z. Zhou, P. Shen, Z. Chen, ACS Nano 3 (2009) 1952.
[16] S.S. Yu, W.T. Zheng, Q.B. Wen, Q. Jiang, Carbon 46 (2008) 537.
[17] S. Dutta, A.K. Manna, S.K. Pati, Phys. Rev. Lett. 102 (2009) 096601.
[18] A. Du, S.C. Smith, J. Phys. Chem. Lett. 2 (2011) 73.
[19] G. Mulas, G. Malloci, C. Joblin, D. Toublanc, Astron. Astrophys. 446 (2006) 537.
[20] P. Oleszczuk, Polish J. Environ. Stud. 12 (2003) 431.
[21] F. Perera, W. Tang, J. Herbstman, D. Tang, L. Levin, R. Miller, S.M. Ho, PLoS ONE 4 (2009) e4488.
[22] K.S. Novoselov, A.K. Geim, S.V. Morozov, D. Jiang, M.I. Katsnelson, I.V. Grigorieva, S.V. Dubonos, A.A. Firsov, Nature Lett. 438 (2005) 197.
[23] P.C. Mishra, A. Yadav, Natl. Acad. Sci. Lett. 35 (2012) 53.
[24] W. Kohn, L. Sham, Phys. Rev. 140 (1965) A1133.
[25] D.H. Ess, K.N. Houk, J. Phys. Chem. A 109 (2005) 9542.

[26] S.F. Sousa, P.A. Fernandes, M.J. Ramos, J. Phys. Chem. A 111 (2007) 10439.
[27] P.J. Silva, M.J. Ramos, Comput. Theoret. Chem. 966 (2011) 120.
[28] Y. Zhao, D.G. Truhlar, J. Phys. Chem. 110 (2006) 5121.
[29] P. Politzer, J.S. Murray, M.C. Concha, Int. J. Quant. Chem. 88 (2002) 19.
[30] P. Politzer, J.S. Murray, Z. Peralta-Inga, Int. J. Quant. Chem. 85 (2001) 676.
[31] A. Kumar, P.C. Mishra, Topics in current chemistry, in: K.D. Sen (Ed.), Molecular Similarity II, vol. 174, Springer-Verlag, Heidelberg, 1995, p. 27.
[32] K.P. Vijayalakshmi, C.H. Suresh, J. Comput. Chem. 29 (2008) 1808.
[33] A.K. Singh, P.C. Mishra, Int. J. Quant. Chem. 107 (2007) 597.
[34] A. Kumar, P.C. Mishra, S. Suhai, J. Phys. Chem. A 110 (2006) 7719.
[35] S. Tiwari, P.K. Shukla, P.C. Mishra, J. Mol. Model. 14 (2008) 631.
[36] N. Agnihotri, P.C. Mishra, J. Mol. Mod. 17 (2011) 1435.
[37] C.G. Mohan, A. Kumar, P.C. Mishra, Int. J. Quant. Chem. 60 (1996) 699.
[38] A. Kumar, A.K. Bhattacharjee, P.C. Mishra, Int. J. Quant. Chem. 43 (1992) 579.
[39] A. Kumar, P.C. Mishra, in: J.S. Murray, K.D. Sen (Ed.), Molecular Electrostatic Potentials: Concepts and Applications, Elsevier, Amsterdam, 1996, p. 257.
[40] S.R. Gadre, P.K. Bhadane, S.S. Pundlik, S.S. Pingale, in: J.S. Murray, K.D. Sen (Ed.), Molecular Electrostatic Potentials: Concepts and Applications, Elsevier, Amsterdam, 1996, p. 219.
[41] C.H. Suresh, S.R. Gadre, J. Org. Chem. 64 (1999) 2505.
[42] P. Politzer, J. Chem. Phys. 72 (1980) 3027.
[43] P.C. Hariharan, J.J. Kaufman, C. Petrongolo, Int. J. Quant. Chem. 20 (1981) 1083.
[44] C.M. Breneman, K.B. Wiberg, J. Comput. Chem. 11 (1990) 361.
[45] U.C. Singh, P.A. Kollman, J. Comput. Chem. 5 (1984) 129.
[46] R.S. Mulliken, J. Chem. Phys. 23 (1955) 1833.
[47] Gaussian 09, Revision A.1, M. J. Frisch, G. W. Trucks, H. B. Schlegel, G. E. Scuseria, M. A. Robb, J. R. Cheeseman, G. Scalmani, V. Barone, B. Mennucci, G. A. Petersson, H. Nakatsuji, M. Caricato, X. Li, H. P. Hratchian, A. F. Izmaylov, J. Bloino, G. Zheng, J. L. Sonnenberg, M. Hada, M. Ehara, K. Toyota, R. Fukuda, J. Hasegawa, M. Ishida, T. Nakajima, Y. Honda, O. Kitao, H. Nakai, T. Vreven, J. A. Montgomery, Jr., J. E. Peralta, F. Ogliaro, M. Bearpark, J. J. Heyd, E. Brothers, K. N. Kudin, V. N. Staroverov, R. Kobayashi, J. Normand, K. Raghavachari, A. Rendell, J. C. Burant, S. S. Iyengar, J. Tomasi, M. Cossi, N. Rega, J. M. Millam, M. Klene, J. E. Knox, J. B. Cross, V. Bakken, C. Adamo, J. Jaramillo, R. Gomperts, R. E. Stratmann, O. Yazyev, A. J. Austin, R. Cammi, C. Pomelli, J. W. Ochterski, R. L. Martin, K. Morokuma, V. G. Zakrzewski, G. A. Voth, P. Salvador, J. J. Dannenberg, S. Dapprich, A. D. Daniels, O. Farkas, J. B. Foresman, J. V. Ortiz, J. Cioslowski, and D. J. Fox, Gaussian, Inc., Wallingford CT, 2009.
[48] GaussView, Version 5, R. Dennington, T. Keith, John Millam, Semichem Inc., Shawnee Mission KS, 2009.
[49] X. Zhang, Q.-S. Li, Y. Xie, H.F. Schaefer III, Mol. Phys. 105 (2007) 2743.
[50] M. Baba, Y. Kowaka, U. Nagashima, T. Ishimoto, H. Goto, N. Nakayama, J. Chem. Phys. 135 (2011) 054305.
[51] A. Ricca, E.L.O. Bakes, C.W. Bauschlicher, Astrophys. J. 659 (2007) 858.
[52] P.C. Mishra, A. Kumar, Int. J. Quant. Chem. 71 (1999) 191.
[53] C.-E. Boström, P. Gerde, A. Hanberg, B. Jernström, C. Johansson, T. Kyrklund, A. Rannug, M. Törnqvist, K. Victorin, R. Westerholm, Environ. Health Perspect. 110 (2002) 451.
[54] H. Rubin, Carcinogenesis 22 (2001) 1903.
[55] E.J.G. Santos, D. Sánchez-Portal, A. Ayuela, Phys. Rev. B 81 (2010) 125433.
[56] G. Xu, C.M. Torres Jr., J. Tang, J. Bai, E.B. Song, Y. Huang, X. Duan, Y. Zhang, K.L. Wang, Nano Lett. 11 (2011) 1082.
[57] G. Brumfiel, Nature 467 (2010) 642.
[58] A.H. Castro Neto, F. Guinea, N.M.R. Peres, K.S. Novoselov, A.K. Geim, Rev. Mod. Phys. 81 (2009) 109.